J. Cell. Mol. Med. Vol 11, No 5, 2007 pp. 1069-1086

Matrix metalloproteinase-2, caveolins, focal adhesion kinase and c-Kit in cells of the mouse myocardium

Woo Jung Cho [a], Ava K. Chow [b], Richard Schulz [b], Edwin E. Daniel [a, *]

[a] *Department of Pharmacology, Faculty of Medicine and Dentistry, University of Alberta, Edmonton, Alberta, Canada*
[b] *Department of Pediatrics and Cardiovascular Research Group, Faculty of Medicine and Dentistry, University of Alberta, Edmonton, Alberta, Canada*

Received: July 10, 2007; Accepted: August 22, 2007

Abstract

Matrix metalloproteinase-2 (MMP-2) may play roles at intracellular and extracellular sites of the heart in ischaemia/reperfusion injury. Caveolins (Cav-1, -2 and -3) are lipid raft proteins which play roles in cell signalling. This study examined, using immunohistochemistry and two photon confocal microscopy, if MMP-2 and caveolins co-localize at the plasma membrane of cardiac cells: cardiomyocytes (CM), fibroblasts (FB) and capillary endothelial cells (CEC) in the left ventricle (LV) of the Cav-$1^{+/+}$ and Cav-$1^{-/-}$ mouse heart. In Cav-$1^{+/+}$ mouse LV MMP-2 and Cav-1 co-localized at CM plasma membranes, and at multiple locations in FB and CEC. MMP-2 co-localized with Cav-2 only at CEC. MMP-2 co-localized with Cav-3 at CM plasma membranes and Z-lines, and partially at FB and CEC. In Cav-$1^{-/-}$ LV Cav-1 and MMP-2 were absent or reduced everywhere. Cav-2 appeared at CEC despite the absence of Cav-1. Cav-3 appeared at CM plasma membranes and Z-lines, FB and CEC. Also, FAK in FB and c-Kit in interstitial Cajal-like cells (ICLC) were completely absent. By transmission electron microscopy in Cav-$1^{+/+}$, regular size caveolae (Cav) were at CEC, irregular size Cav were at CM and a few were at FB. In Cav-$1^{-/-}$ there were few Cav at CM and FB and some at CEC. To conclude, MMP-2 is closely associated with caveolins at FB and CEC as well as at CM. Also, MMP-2 is closely associated with FAK at FB and c-Kit at ICLC. Thus, Cav-1 expression is not necessary for Cav-2 expression. Cav-3 or Cav-3 with Cav-2 has the capability to make Cav.

Keywords: cardiomyocyte • fibroblast • capillary endothelial cell • interstitial cajal-like cell • matrix metalloproteinase-2 • caveolins • focal adhesion kinase • von Willebrand Factor • c-Kit

Introduction

In earlier histological and immunohistochemical observations of cardiac muscle, its cardiomyocytes (CM) were found to be closely related structurally to fibroblasts (FB), capillary endothelial cells (CEC) and other components in the interstitial space in the heart tissue [1–5]. However, the relationships between proteins in these structures using histology or immunocytochemistry were left unclear. Marker proteins for CM (*e.g.* myomesin and caveolin-3) [1, 6, 7], FB (*e.g.* vimentin, discoidine domain receptor-2, α-smooth muscle actin and focal adhesion kinase) [6, 8, 9, 10] and CEC (*e.g.* von Willebrand factor) [11, 12] were examined to identify cell type. However, the interpretation of localization and co-localization of different membrane proteins is difficult when complexes of CM, FB and CEC are closely aligned as they are in the myocardium.

*Correspondence to: E. E. DANIEL,
Room 9-10, Medical Sciences Building, Department of Pharmacology, Faculty of Medicine and Dentistry, University of Alberta, Edmonton, Alberta T6G 2H7, Canada
Tel.: +17 80 49 22 10 5
Fax: +17 80 49 24 32 5
E-mail: edaniel@ualberta.ca

doi: 10.1111/j.1582-4934.2007.00113.x

Matrix metalloproteinase-2 (MMP-2) (gelatinase A, type II collagenase) is a constitutive enzyme that is ubiquitously expressed at a higher level than any other MMP [13]. MMP-2 may play important roles in wound healing and heart failure at both intracellular and extracellular matrix of the heart in ischaemia / reperfusion injury [13–15]. MMP-2 has been recently shown to be localized at CM plasma membranes, Z-lines and myofilaments [16] and co-localized with caveolin-1 at surface of the human endothelial cells [17]. Its existence and localization with other proteins in FB and related cells is unknown.

Caveolins are structural proteins that insert in the plasmalemma to form caveolae (Cav), major components of lipid raft with cholesterols, sphingolipids and G-proteins in smooth muscle cells (SMCs) [19–24] and other cells [25]. Caveolins have three isoforms: caveolin-1 (Cav-1), caveolin-2 (Cav-2) and caveolin-3 (Cav-3). Each isoform has a caveolin scaffolding domain (CSD: 82–101 amino acid of Cav-1, 54–73 amino acid of Cav-2 and 55–74 amino acid of Cav-3) that can bind to signalling molecules and play crucial roles in cell signal transduction [18].

We previously reported that Cav-1 localized at CM membrane and co-localized with MMP-2 by confocal microscopy and immunofluorescent intensity analysis [16]. The first objective of this study is to expand our previous report to show the localizations and co-localizations of MMP-2, caveolin isoforms (Cav-1, Cav-2 and Cav-3), in CM, FB, and CEC in the left ventricular (LV) myocardium of Cav-$1^{+/+}$ and Cav-$1^{-/-}$ mouse heart. Studies of the distributions of focal adhesion kinase, discoidine domain receptor-2, von Willebrand factor and tyrosine kinase receptor were used to identify FB, endothelial cells and interstitial cells of Cajal (ICC) related cells. We used 2-dimensional (2D) and 3-dimensional (3D) confocal microscopy among. As there are no 3D confocal microscopic observations to clarify the stereological associations among proteins in CM, FB and CEC, we examined 5 μm cyosections for 2D confocal microscopic study and 20 μm cryosections for 3D study with two-photon confocal microscopy. The second objective is to compare location and distribution of cells and their organelles using electron microscopy in CM, FB and CEC.

Materials and methods

Immunohistochemical study

Tissue preparation

5 Cav-$1^{+/+}$ mice (B6 129 SF2/J, 6-8 week old male) purchased from Jackson Laboratories (Bar Harbor, Maine, USA) were the control group. 5 Cav-$1^{-/-}$ mice (cav<tm 1 M Is>J, 6-8-week-old male) from our breeding colony were the experimental group. All mice were sacrificed by cervical dislocation according to a protocol approved by the University of Alberta Animal Care Committee and following the guidelines of Canada Council on Animal Care. The hearts were rapidly excised and perfused via the aorta [16], followed by fixed in 4% paraformaldehyde (PFA) in 0.1 M sodium phosphate buffer (PB, pH 7.2–7.4) for 4 hrs at 4°C. The fixed hearts were rinsed and cryoprotected in 30% sucrose in 0.1 M PB overnight at 4°C and then stored at –80°C.

Cryosection

The cryoprotected hearts were put into disposable embedding molds (Cat. No. 18646A, Polysciences, Inc., Warrington, PA, USA) and filled with Tissue-Tek® optimal cutting temperature (O.C.T.) compound. They were frozen on the pre-cooler of the cryostat for 1 hr. The frozen hearts were cryosectioned in 5 μm thickness for 2D images and 20 μm thickness for 3D images. The heart cryosections were attached to glass slides coated with 1.5% 3-aminopropyltriethoxysilane (Cat. No. A-3648, Sigma Chemical Co., St. Louis, MO, USA) in acetone. The cryosections were dried for 15 min. at room temperature.

Double-immunofluorescent labelling

The dried 5 μm cryosections were first rinsed in 0.3% Triton-X 100 (TX-100) in phosphate buffered saline (PBS, pH 7.2–7.4) and the dried 20 μm cryosections were rinsed in 0.5 % TX-100 in PBS to remove O.C.T. compound and accelerate antibody penetration into the target antigen. They were then rinsed in PBS. To reduce artificial staining of non-specific proteins, 10 % normal donkey serum was applied before applying primary antibody. For co-localization study of two different proteins, double immunolabelling was accomplished by one of two different methods; either (1) Double labelling of primary antibodies from the different host species and (2) Double labelling of primary antibodies from the same host species, as previously described [24]. Sequential staining of each primary antibody provided the best results and was performed in the two different methods. Endogenous mouse IgG in mouse tissue was blocked by mouse IgG blocking reagent of M.O.M.™ kits (Cat. No. BMK-2202, Vector Laboratories, Inc., Burlingame, CA, USA).

All antibodies and sera used are summarized in Table 1. During the incubation with all antibodies, 2% normal donkey serum of total incubation volume was added. All experimental procedures were performed at room temperature, 22±1°C. To determine specificity of immunolabelling, primary antibody was omitted, or when the antigen was available, it was used to saturate the primary antibody.

Table 1 Antibodies and sera

Antibody	Host	Dilution	Cat. No.	Source
Primary antibodies				
MMP-2	Mouse	1:400	MAB3308	Chemicon International
Cav-1	Mouse	1:50	610406	BD transduction
Cav-2	Rabbit	1:400	ab2911	Abcam
Cav-3	Mouse	1:200	610420	BD transduction
Cav-3	Rabbit	1:200	ab2912	Abcam
FAK	Mouse	1:100	MAB1144	Chemicon International
DDR2	Rabbit	1:10	ab5520	Abcam
vWF	Rabbit	1:200	AB7356	Chemicon International
c-Kit	Mouse	1:20	32-9000	Invitrogen
Secondary or tertiary antibodies				
Fab fragment rabbit antimouse IgG			325-007-003	Jackson ImmunoResearch
Cy3-donkey antimouse IgG			715-165-151	Jackson ImmunoResearch
Alexa488-donkey antirabbit IgG			A-21206	Invitrogen
Sera				
Mouse IgG blocking reagent			BMK-2202	Vector
Normal donkey serum			566460	Calbiochem

MMP-2, matrix metalloprotenase-2; Cav-1, caveolin-1; Cav-2, caveolin-2; Cav-3, caveolin-3; FAK, focal adhesion kinase; DDR2, discoidin domain receptor-2; vWF, von Willebrand factor; c-Kit, receptor tyrosine kinase

Laser lines for confocal microscopic study

The immunolabelled cryosections were observed by two photon confocal microscope (LSM 510, Carl Zeiss Co., Jena, Germany) and saved by LSM 5 Image (Carl Zeiss Co., Jena, Germany). Cy3 (red) was scanned by helium / neon laser (wavelength 543 nm laser line) with long path 590 filter (560–700 nm excitation). Alexa488 (green) was captured by Argon laser (wavelength 488 nm laser line) with band path 500–550 IR filter (500–550 nm excitation). DAPI (blue) for nuclei staining of all cells was obtained in range of 400–470 nm excitation. All images obtained from confocal microscope were enhanced by brightness, contrast and γ tool of LSM 5 image. Some of them were deconvoluted by AutoDeblur and AutoVisualize (Media Cybernetics Inc., Bethesda, MD, USA).

Ultrastructural study

Two Cav-$1^{+/+}$ and 2 Cav-$1^{-/-}$ mice (6-8-week-old male) were examined for ultrastructural study. The mouse was deeply anaesthetized with halothane and the thorax opened. The heart was freed from the pericardium and a 26G1/2 needle (Reorder No. 305111, Becton Dickinson & Co., Franklin Lakes, NJ, USA) inserted into the left ventricle. The right auricular appendage was cut and the mouse was exsanguinated by flushing its circulatory system with 30 ml of 0.1 M PB, followed by 30 ml of mixture of 0.1% glutaraldehyde (GA) and 2% PFA in 0.1 M PB. The partially fixed heart was removed and cut to 1 mm^3 and placed in mixture of 2.5% GA and 4% PFA in 0.075 M sodium cacodylate buffer (CB) for a further 2 hrs at 4°C. The fixed heart samples were shortly rinsed in 0.075 M CB, followed by post-fixed in 1% OsO_4 (Cat. No. 19152, Electron Microscopic Sciences, Washington, PA, USA) in 0.05 M CB for 2 hrs at 4°C. The

Table 2 Immunofluorescent intensity of proteins in Cav-1$^{+/+}$ and Cav-1$^{-/-}$ mouse left ventricular myocardium

	MMP-2	Cav-1	Cav-2	Cav-3	FAK	DDR2	vWF	c-kit
Cav-1$^{+/+}$ Mouse left ventricular myocardium								
CM PM	++	++	-	+++	-	-	-	-
Z-lines	+++	+	-	+++	-	-	-	-
MF	++	+	-	+++	-	-	-	-
FB	+++	+++	-	+	+++	++	-	+/-
CEC	+++	+++	+++	++	-	-	+++	-
ICLC	-	-	-	-	-	-	-	+++
Cav-1$^{-/-}$ Mouse left ventricular myocardium								
CM PM	+/-	-	-	+++	-	-	-	-
Z-lines	+/-	-	-	+++	-	-	-	-
MF	+/-	-	-	+++	-	-	-	-
FB	+/-	-	-	+	-	++	-	-
CEC	-	-	+++	++	-	-	+++	-
ICLC	-	-	-	-	-	-	-	-

CM, cardiomyocytes; FB, fibroblasts; CEC, capillary endothelial cells; ICLC, interstitial Cajal-like cells; PM, plasma membranes; MF, myofilaments; MMP-2, matrix metalloprotenase-2; Cav-1, caveolin-1; Cav-2, caveolin-2; Cav-3, caveolin-3; FAK, focal adhesion kinase; DDR2, discoidin domain receptor-2; vWF, von Willebrand factor; c-Kit, receotor tyrosine kinase; +, ++ and +++ indicate intensity of immunoreactivity; - means absent or inconspicuous; +/- means present occasionally.

pre- and post-fixed heart samples were dehydrated using ethyl-alcohol substitution with propylene oxide, and infiltrated using a mixture of Araldite512-Embed812. The samples were heat polymerized with an accelerator 1.5% DMP-30 (2,4,6-tri-(dimethylaminomethyl) phenol) (Cat. No. 13600, Electron Microscopic Sciences, Washington, PA, USA) for 48 hrs at 60°C. Semi-thin sections of 1 μm were cut, stained with 1% toluidine blue and evaluated for ultra-thin section. Ultra-thin sections of 50 nm were cut, loaded using perfect loop (Cat. No. 70944, Electron Microscopic Sciences, Washington, PA, USA) on 300-mesh copper grid or 100-mesh copper grids coated with 0.25% formvar solution in ethylene dichloride (Cat. No. 15810, Electron Microscopy Sciences, USA). Sections were stained with 4% uranyl acetate (Cat. No. CU001-1, Canemco & Marivac Inc., QC, Canada) in 50% ethanol and Reynold's lead citrate, lead nitrate (Cat. No. L005, TAAB Laboratories Equipment Ltd., Berks, PA, USA) and sodium citrate (Cat. No. 3646-01, J. T. Baker Inc., Phillipsburg, NJ, USA). The grids were examined in a Philips 410 electron microscope equipped with a charge-coupled device camera (MegView III) at 80 kV.

Results

General distribution of MMP-2

In the Cav-1$^{+/+}$ mouse LV myocardium (LVM), MMP-2 was widely and prominently distributed at CM plasma membrane and Z-lines, FB plasma membrane and cytoplasm, and CEC plasma membrane and cytoplasm. In Cav-1$^{-/-}$ mouse LVM, MMP-2 was significantly reduced or absent, everywhere.

MMP-2 and caveolins in cardiomyocyte

Co-localizaton of MMP-2 and Cav-1

MMP-2 co-localized well with Cav-1 at the CM plasma membrane, FB and CEC, and partially at the Z-lines in Cav-1$^{+/+}$ mouse LVM (Fig. 1A–C). In Cav-1$^{-/-}$

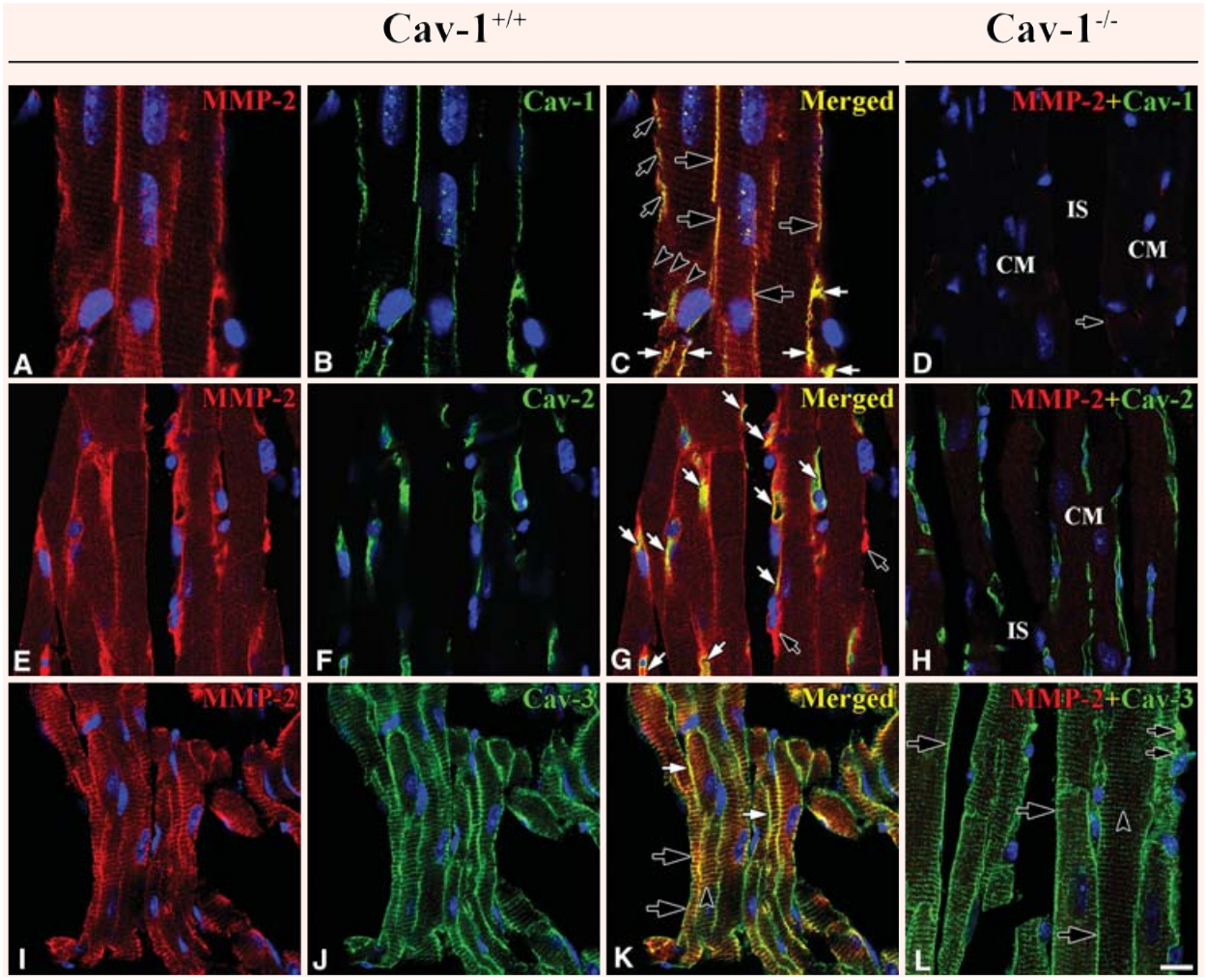

Fig. 1 Co-localization of MMP-2 and Caveolins in Cav-$1^{+/+}$ and Cav-$1^{-/-}$ mouse LVM. In Cav-$1^{+/+}$ MMP-2 (red) appeared to have good co-localization with Cav-1 (green) at CM plasma membranes (large open arrows), CEC (closed arrows) and FB (small open arrows), and partial co-localization occurs at **Z-lines** (open arrowheads) **(A–C)**. MMP-2 (red), however, appeared to have good co-localization with Cav-2 (green) only at CEC (closed arrows). FB with MMP-2 appear (open arrows) **(E–G)**. MMP-2 (red) appeared to have good co-localization with Cav-3 (green) at CM plasma membranes (open arrows) and **Z-lines** (arrowhead), and partial co-localization at FB (closed arrows) **(I–K)**. In Cav-$1^{-/-}$ Cav-1 is absent and MMP-2 is markedly reduced at CM plasma membrane (arrow), CEC and FB **(D)**. IS refers to interstitial space. Interestingly, Cav-2 (green) appears regardless of Cav-1 only at CEC **(H)** and Cav-3 (green) appears at CM plasma membranes (large arrows), **Z-lines** (arrowhead), and FB (small arrows) like in Cav-$1^{+/+}$ **(I)**. CM is cardiomyocyte and IS is interstitial space. Scale bar is 10 mm for A–H and I, and 20 mm for I–K.

mouse LVM, MMP-2 was significantly reduced or absent in all these cells (Fig. 1D).

Co-localization of MMP-2 and Cav-2

The distribution of Cav-2 was completely different from that of Cav-1 in CM plasma membrane. In Cav-$1^{+/+}$ mouse LVM Cav-2 was present only at CEC: long narrow tubular and anastomotic structures shown in optimal longitudinal section), but there was no Cav-2 at the CM plasma membrane and Z-lines. MMP-2 co-localized well with Cav-2 at the CEC. A few cells adjacent to the CM plasma membrane in interstitial space were MMP-2-positive, but Cav-2-negative. It was unclear whether FB or another cell has MMP-2 (Fig. 1E–G). In Cav-$1^{-/-}$ mouse LVM,

interestingly, Cav-2 was still present regardless of Cav-1 at CEC, but there was none at the CM plasma membrane and Z-lines (Fig. 1H).

Co-localization of MMP-2 and Cav-3

The CM marker protein, Cav-3, in Cav-$1^{+/+}$ mouse LVM was prominently present and co-localized well with MMP-2 at CM plasma membrane and Z-lines (Fig. 1I–K). In Cav-$1^{-/-}$ mouse LVM Cav-3 was present at CEC and FB, identified as having a comparatively bigger nucleus and narrower cytoplasm than CEC, as well as at CM membrane and Z (Fig. 1I).

MMP-2 in fibroblast

FAK-positive fibroblast and co-localization with MMP-2

FAK immunoreactivity appeared at FB which ran alongside CM and CEC. In Figure 2A–C, one FAK-positive FB (FAK-FB) was connected to another FAK-FB by an elongated thin tail. MMP-2 appeared in the FAK-positive FB and co-localized with FAK in Cav-$1^{+/+}$ mouse LVM (Fig. 2A–C). On the other hand, in Cav-$1^{-/-}$ mouse LVM, FAK was absent at FB (Fig. 2D).

DDR-2-positive fibroblast and co-localization with MMP-2

To further clarify the relationships of proteins in FB, we used discoidin domain receptor-2 (DDR-2) as a marker. It specifically appeared at FB located in interstitial spaces and also appeared faintly and probably non-specifically in CM. MMP-2 appeared in DDR-2-positive FB (DDR-2-FB) and partially co-localized with DDR-2 in Cav-$1^{+/+}$ mouse LVM (Fig. 2E–G). As well, in Cav-$1^{-/-}$ mouse LVM, DDR-2 appeared in FB located in the interstitial space (Fig. 2H).

MMP-2 in capillary endothelial cell

vWF-positive capillary endothelial cell and co-localization with MMP-2

von Willebrand factor (Vwf) appeared in CEC over the LVM of both Cav-$1^{+/+}$ and Cav-$1^{-/-}$ mouse LVM. There was no difference in vWF distribution between two strains. MMP-2 appeared at vWF-positive CEC (vWF-CEC) and co-localized with vWF in the Cav-$1^{+/+}$ mouse LVM, but not in the Cav-$1^{-/-}$ LVM (Fig. 2I–L).

MMP-2 in interstitial Cajal-like cell

c-Kit-positive Interstitial Cajal-like Cell and co-localization with MMP-2

c-Kit-positive interstitial Cajal-like cells (c-Kit-ICLC) appeared as a group in certain areas in interstitial space nearby CM and CEC. The c-Kit-ICLC ran parallel to or twisted around CEC. MMP-2 appeared at c-Kit-ICLC and co-localized with c-Kit in Cav-$1^{+/+}$ mouse LVM (Fig. 2M–O). In Cav-$1^{-/-}$ mouse LVM, not only was MMP-2 significantly reduced or absent, but also c-Kit immunoreactivity was completely absent. (Fig. 2P).

Caveolin isoforms in cardiomyocyte, fibroblast, capillary endothelial cell and interstitial Cajal-like cell

Co-localization of Cav-1 and Cav-2

As noted above, Cav-1 immunoreactivity appeared at plasma membranes and around Z-lines of CM, at FB and at CEC of Cav-$1^{+/+}$ mouse LVM. Cav-1 immunoreactivity co-localized with Cav-2 only at CEC. 3D structure of FB with Cav-1 and CEC with Cav-2 showed that these cells twisted around each other and all were closely related (Fig. 3A–C). Cav-2 immunoreactivity appeared at CEC of Cav-$1^{-/-}$ mouse LVM similar to that of Cav-$1^{+/+}$ mouse LVM (Fig. 3D).

Co-localization of Cav-1 and Cav-3

Cav-1 immunoreactivity co-localized well with Cav-3 immunoreactivity at some CM membranes, FB and CEC of Cav-$1^{+/+}$ mouse LVM. Interestingly, the patterns of Cav-1 and Cav-3 immunoreactivities in Z-lines differed. Cav-3 appeared at Z-lines, but Cav-1 appeared as small punctate sites at or near Z-lines (Fig. 3E–G). In Cav-$1^{-/-}$ mouse LVM Cav-3 appeared clearly at CM plasma membranes and Z-lines of CM, at some FB and at some CEC (Fig. 3H).

Co-localization of Cav-2 and Cav-3

Cav-2 immunoreactivity appeared in tubular-shaped and sometimes anastomotic structures, identified as CEC. It was partially co-localized with Cav-3 immunoreactivity in both Cav-$1^{+/+}$ and Cav-$1^{-/-}$ mouse LVM (Fig. 3I–L).

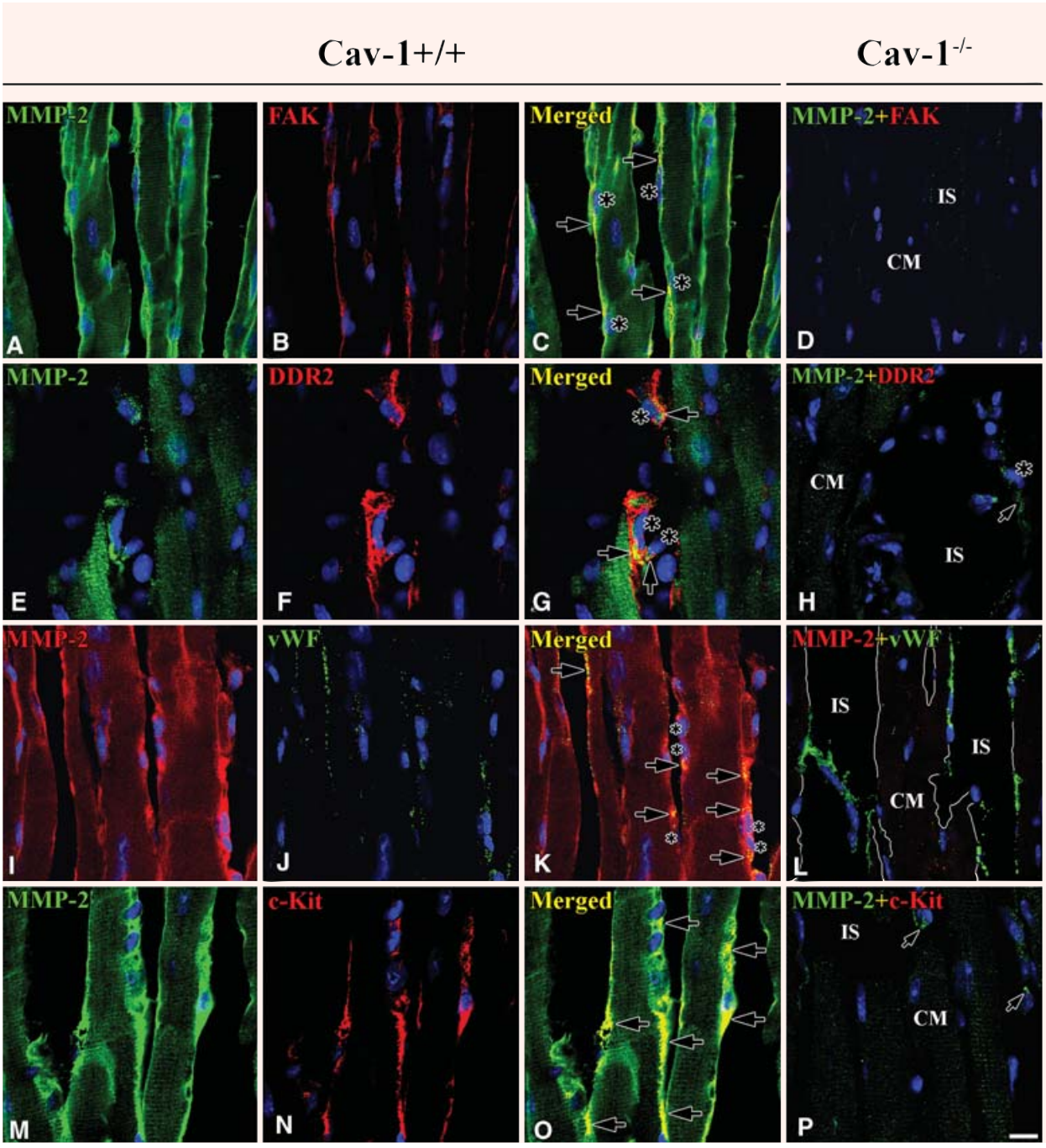

Fig. 2 Co-localization of MMP-2 and FAK / DDR-2 / vWF / c-Kit in Cav-$1^{+/+}$ and Cav-$1^{-/-}$ mouse LVM. In Cav-$1^{+/+}$ co-localization (arrows) of MMP-2 (green) and FAK (red) **(A–C)**, MMP-2 (green) and DDR-2 (red) **(E–G)**, and MMP-2 (red) and vWF (green) **(I–K)** shows that MMP-2 localizes at FB (nucleus: large asterisks) as well as at CEC (nucleus: small asterisks). MMP-2 (green) also co-localizes (arrows) with c-Kit (red) at ICLC near by CM ***(M-N)***. In Cav-$1^{-/-}$, surprisingly, FAK (red) and c-Kit (red) are completely absent at FB and ICLC, respectively, except FAK in nuclei of all cells **(D and P)**. vWF, however, is still present at CEC **(I)**. CM is cardiomyocyte and IS is interstitial space. Scale bar is 10 mm for all images.

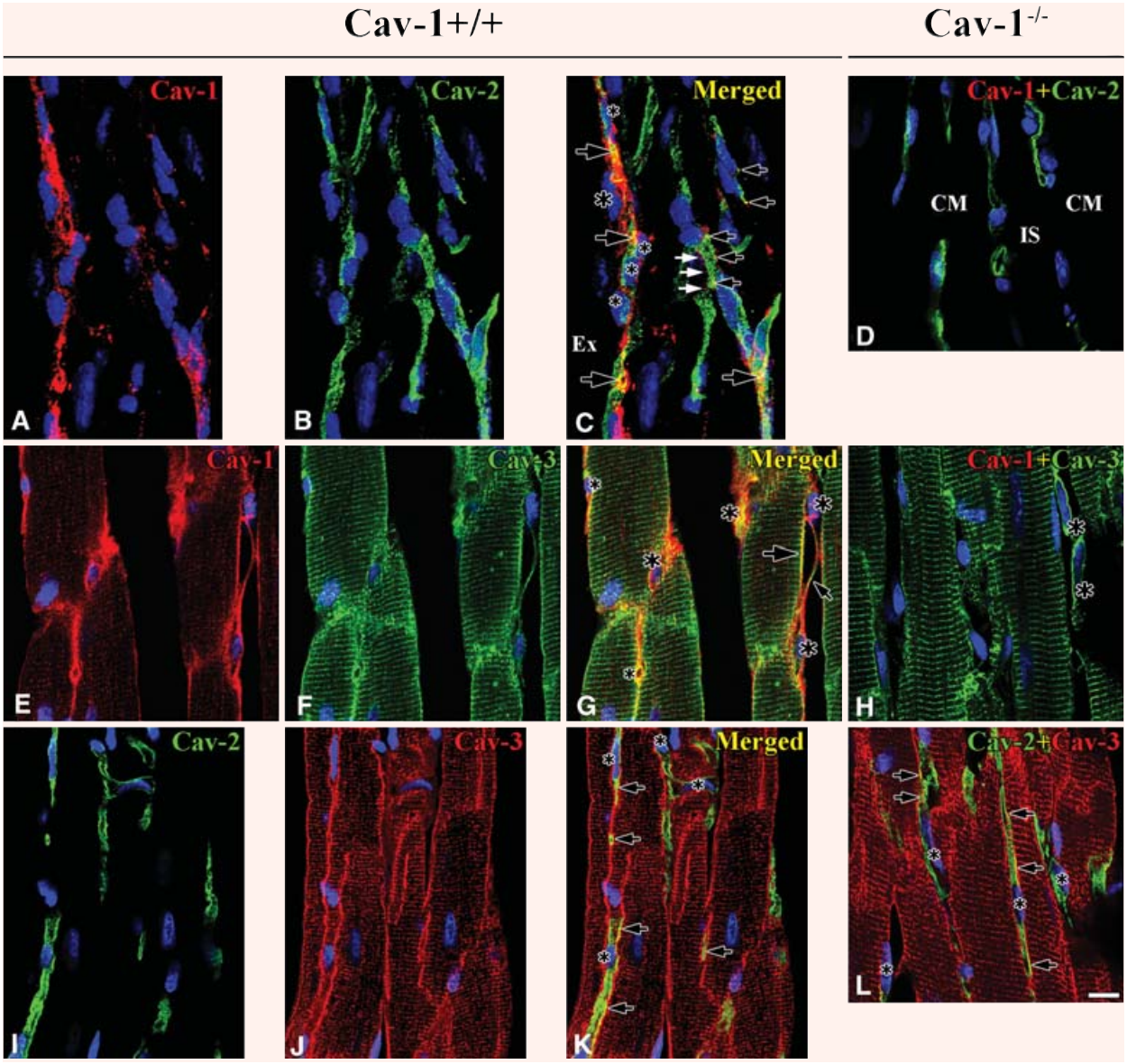

Fig. 3 Co-localization between caveolins in Cav-$1^{+/+}$ and Cav-$1^{-/-}$ mouse LVM. In Cav-$1^{+/+}$ 3D reconstructed images (-45° rotation of y-axis) shows Cav-1 (red) localizes at both FB (nucleus: large asterisks) and CEC (nucleus: small asterisks), but Cav-2 (green) localizes only at CEC. Partial co-localization of Cav-1 and Cav-2 occurs at CEC (open arrows), but sometimes Cav-1 without Cav-2 occurs at CEC membrane (closed arrows) **(A–C)**. Cav-1 (red) co-localizes well with Cav-3 (green) at CM plasma membrane (large open arrow), FB (nucleus: large asterisks) interconnecting with tails (small open arrow) and CEC (nucleus: small asterisks). Also, Cav-1 immunoreactivity occurs near CM **Z-lines** and partial co-localization with Cav-***3*** **(E–G)**. Cav-2 (green) co-localizes partially with Cav-3 (red) at CEC (arrows). CEC make frequently anastomotic structure (asterisk) **(I–K)**. In Cav-$1^{-/-}$ Cav-2 (green) immunoreactivity occurs regardless of Cav-1 at CEC (d). Cav-3 (green), immunoreactivity occurs also at CM plasma membranes, **Z-lines** and FB (asterisks) **(H)**. Co-localization (open arrows) of Cav-2 (green) and Cav-3 (red) at CEC is similar to that in Cav-$1^{+/+}$ **(I)**. CM is cardiomyocyte and IS is interstitial space. Scale bar is 10 mm for all images.

FAK-positive fibroblast and its co-localization with Cav-1

FAK immunoreactivity appeared over all the cytoplasm including elongated cytoplasmic tails of FBs. It co-localized with Cav-1 immunoreactivity in Cav-$1^{+/+}$ mouse LVM. Some FAK-positive FBs (FAK-FB) connected to other FAK-FBs (Fig. 4A–C). In Cav-$1^{-/-}$ mouse LVM, surprisingly, FAK was totally absent except in some nuclei of all type of cells (Fig. 4D).

vWF-positive capillary endothelial cell and its co-localization with Cav-1

Cav-1 localized at both the plasma membrane and cytoplasm of CEC, while vWF usually localized less diffusely at the cytoplasm and co-localized well with Cav-1 where present. One possibility is that vWF is associated with Cav-1 in Cav undergoing endocytosis in the CEC. Co-localization of Cav-1 and vWF demonstrated that Cav-1 is present in CEC in Cav-$1^{+/+}$ mouse LVM (Fig. 4E–G). Regardless of the absence of Cav-1, vWF was also present in CEC in Cav-$1^{-/-}$ mouse LVM (Fig. 4H).

DDR-2-positive fibroblast and its co-localization with Cav-1

In this experiment, DDR-2 immunoreactivity showed better in cross sectioned CM than in longitudinal sectioned CM. Although the number of DDR-2-positive FB (DDR-2-FB) was small, the DDR-2-FB were found in interstitial space and partially co-localized with Cav-1 in Cav-$1^{+/+}$ mouse LVM (Fig. 4I–K). DDR-2-FB also appeared in the interstitial space in Cav-$1^{-/-}$ mouse LVM (Fig. 4I).

c-Kit-positive interstitial cajal-like cell and Its co-localization with Cav-1

c-Kit-positive interstitial Cajal-like cell (c-Kit-ICLC) revealed long thin multiple process and its immuoreactivity co-localized well with that of Cav-1 in Cav-$1^{+/+}$ mouse LVM (Fig. 4M–O). Both Cav-1 and c-Kit were completely absent in Cav-$1^{-/-}$ mouse LVM (Fig. 4P).

FAK-positive fibroblast and its relationship with Cav-2

3D reconstructed images in Figure 5A–C revealed that FAK-FB was positioned close to CEC with Cav-2, but there was no co-localization between two proteins in Cav-$1^{+/+}$ mouse LVM. Figure 5d revealed the presence only of Cav-2 in the non-nuclear components of cells in Cav-$1^{-/-}$ mouse LVM.

c-Kit-positive interstitial Cajal-like cell and its relationship with Cav-2

c-Kit-ICLC appeared in the interstitial space nearby CM. It was not found with Cav-2 in CEC of Cav-$1^{+/+}$ mouse LVM (Fig. 5E–G). Again, c-Kit was completely absent in Cav-$1^{-/-}$ mouse LVM (Fig. 5H).

FAK-positive fibroblast and its co-localization with Cav-3

Both FAK-FB and FAK-negative cells were present in the interstitial space. Only a few of FAK-FBs also contained Cav-3, which was co-localized with FAK. The FAK-negative cells were all Cav-3-positive cells. The FAK-negative Cav-3-positive cells might be DDR-2-FB or c-Kit-FB in Cav-$1^{+/+}$ mouse LVM (Fig. 6A–C). FAK was absent in non-nuclear portions of cells but Cav-3 appeared at FB in interstitial space in Cav-$1^{-/-}$ mouse LVM (Fig. 6D).

DDR-2-positive fibroblast and Its co-localization with Cav-3

A few DDR-2-FB were present in the interstitial space and DDR-2 immunoreactivity was occasionally co-localized with Cav-3 immunoreactivity (Fig. 6E–G). Several weakly DDR-2 positive processes were present around CM in the interstitial space, but there was no co-localization with Cav-3. DDR-2 immunoreactivity also appeared non-specifically in CM of Cav-$1^{-/-}$ mouse LVM (Fig. 6H).

vWF-positive capillary endothelial cell and its relationship with Cav-3

vWF appeared only at CEC and it was not co-localized with Cav-3. This result showed that vWF is closely associated with Cav-1 but not with Cav-3 in both Cav-$1^{+/+}$ and Cav-$1^{-/-}$ mouse LVM (Fig. 6I–L).

c-Kit-positive interstitial Cajal-like cell and its co-localization with Cav-3

Cav-3 also appeared at ICLC where it was partially co-localized with c-Kit. The co-localization usually

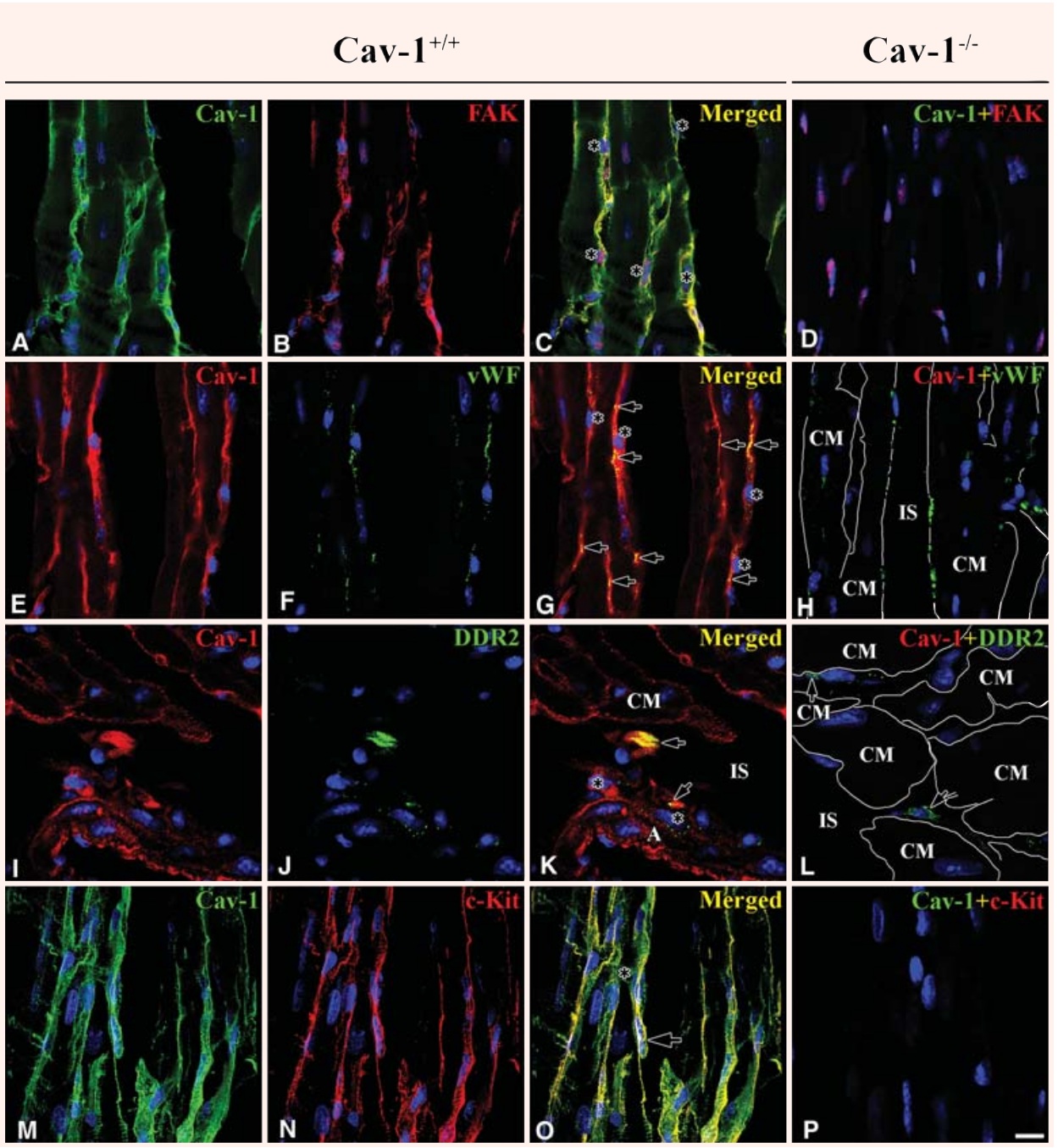

Fig. 4 Co-localization of Cav-1 and FAK / DDR-2 / vWF / c-Kit in Cav-$1^{+/+}$ and Cav-$1^{-/-}$ mouse LVM. In Cav-$1^{+/+}$ Cav-1 (green) co-localized well with FAK (red) at FB with long tails (nucleus: asterisks) **(A–C)**. Cav-1 (red), also, co-localized (arrows) well with vWF (green) at CEC (nucleus: asterisks) **(E–G)**. Cav-1 (red) co-localized (arrows) with DDR-2 (green) at a few FB around venule but didn't co-localize at some FB (asterisks) **(I–K)**. Also, Cav-1 (green) co-localized well with c-Kit (red) **(M–O)**. In Cav-$1^{-/-}$ FAK and c-Kit disappear completely with Cav-1 at FB and ICLC, respectively **(D and P)** . However, vWF (green) and DDR-2 (green) appear at CEC and FB, respectively **(H and I)**. CM is cardiomyocyte and IS is interstitial space. Scale bar is 10 mm for all images.

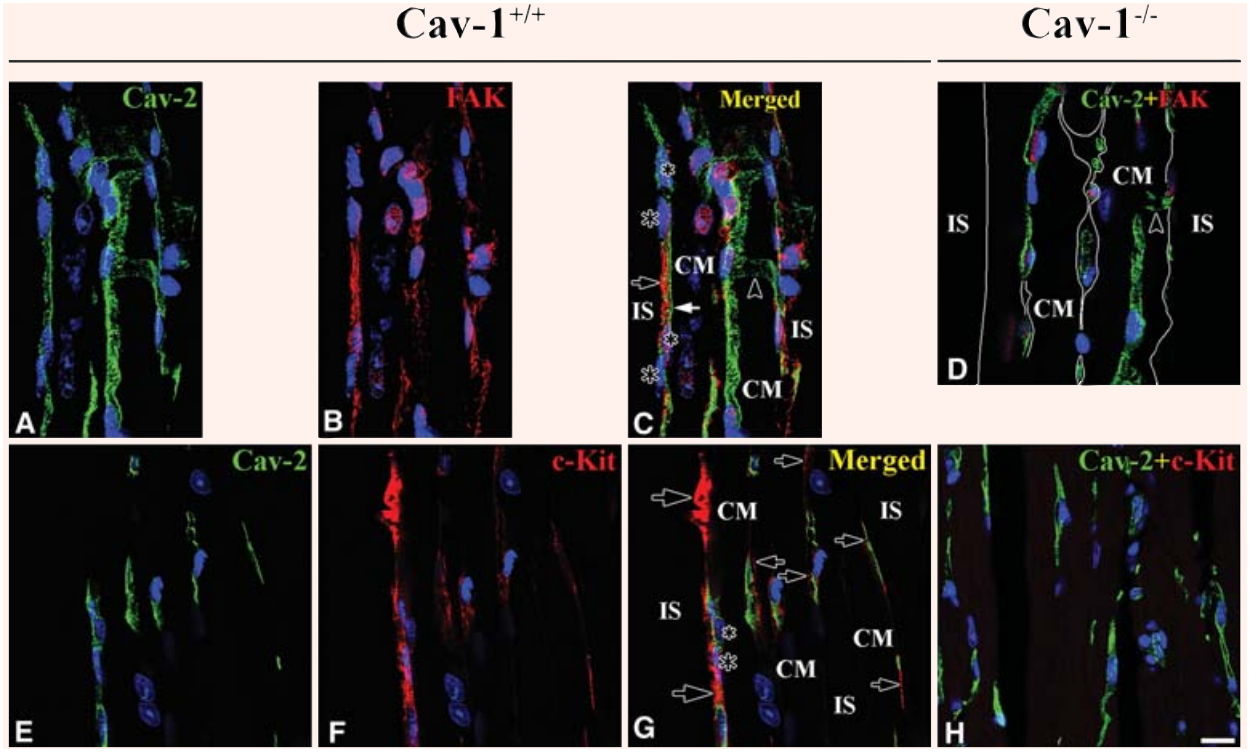

Fig. 5 Co-localization of Cav-2 and FAK / c-Kit in Cav-1$^{+/+}$ and Cav-1$^{-/-}$ mouse LVM. In Cav-1$^{+/+}$ Cav-2 (green) (closed arrow) appears only at CEC (nucleus: small asterisks) and FAK (red) (open arrow) only at FB (nucleus: large asterisks). An anastomotic structure appears (open arrowhead) **(A–C)**. Cav-2 (green) doesn't co-localize with c-Kit (red). Arrow indicates for FB, large asterisk for FB nucleus and small asterisk for CEC nucleus **(E–G)**. In Cav-1$^{-/-}$ FAK and c-Kit are missing with Cav-1 **(D and H)**. CM is cardiomyocyte and IS is interstitial space. Scale bar is 10 mm for all images.

appeared at ICLC processes. The ICLC processes were very close to CM membranes making it hard to distinguish Cav-3 positive ICLC processes from Cav-3 positive CM plasma membranes in Cav-1$^{+/+}$ mouse LVM (Fig. 6M–O). c-Kit was completely absent but Cav-3 appeared clearly at CM membranes, Z-lines and FB in Cav-1$^{-/-}$ mouse LVM (Fig. 6P).

Non-association between FAK and vWF

An experiment to determine if FAK and vWF were ever present in the same cell was essential to determine that these markers discriminated between FB and CEC. FAK was found to be present specifically at FB and non-specifically at nuclei of all cell types of Cav-1$^{+/+}$ mouse LVM (Fig. 7A–C). Moreover, vWF was specifically present at CEC and endothelial cell of both Cav-1$^{+/+}$ and Cav-1$^{-/-}$ mouse LVM (Fig. 7D).

Association between DDR-2 and c-Kit

As a rule, DDR-2-FB and c-Kit-ICLC immunoreactivities appeared in the interstitial space in distinct cells. However, a few FB possessed both DDR-2 and c-Kit and the two proteins partially co-localized in Cav-1$^{+/+}$ mouse LVM (Fig. 7E–G). Although c-Kit was completely absent, DDR-2-FB appeared in Cav-1$^{-/-}$ mouse LVM (Fig. 7H).

Ultrastructural observation

Cardiomyocyte

In longitudinal sections of CM of Cav-1$^{+/+}$ mouse LVM CM revealed some opened Cav, flask-shaped invaginations at the sarcolemma. An abundance of large mitochondria interrupted myofilaments without clearly defined limits. Well-developed sarcoplasmic reticulum (SR) was arranged continuously along sar-

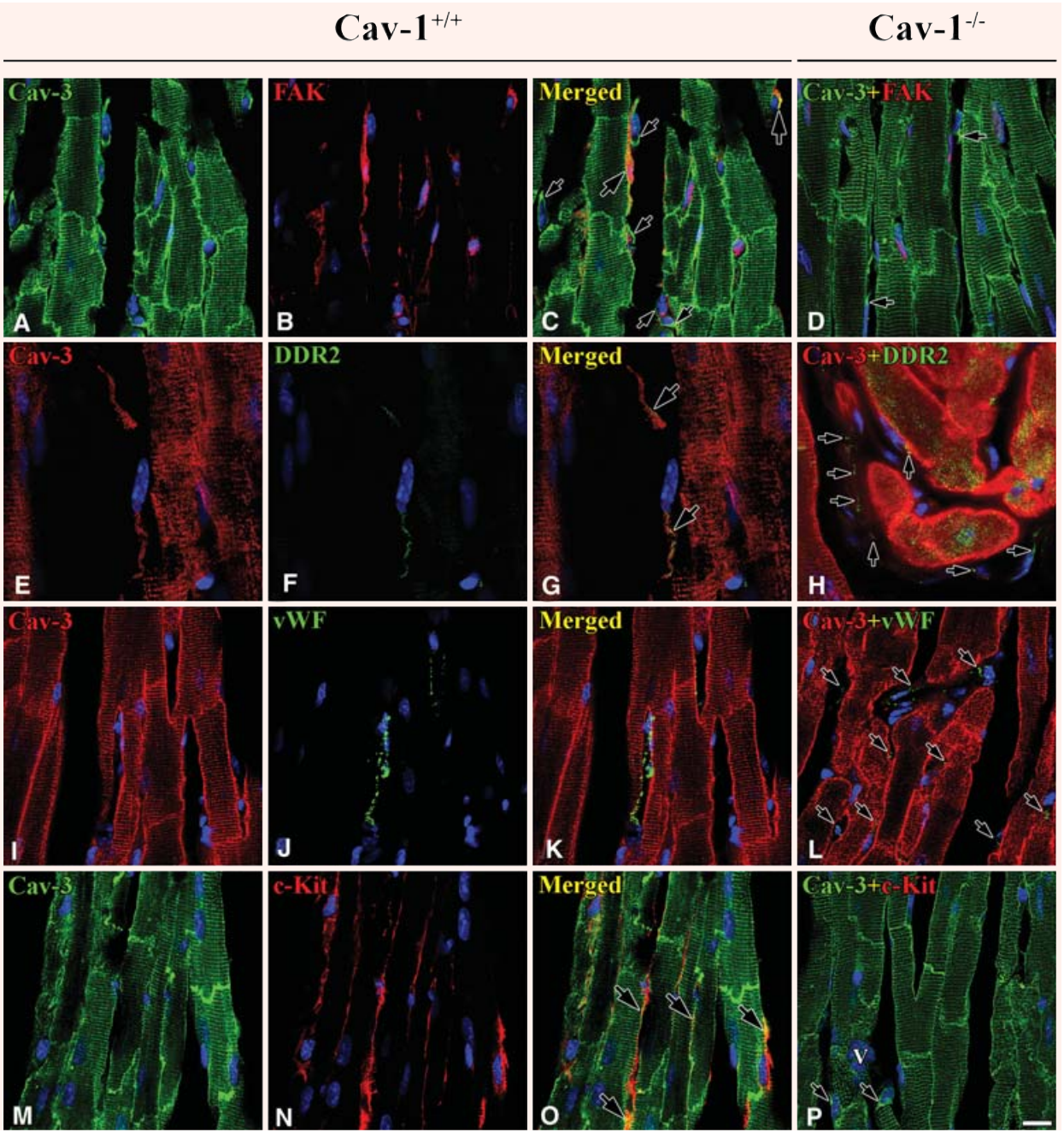

Fig. 6 Co-localization of Cav-3 and FAK / DDR-2 / vWF / c-Kit in Cav-$1^{+/+}$ and Cav-$1^{-/-}$ mouse LVM. In Cav-$1^{+/+}$ mouse some FB are Cav-3- (green) and FAK-positive (red) and the two proteins are partially co-localized (yellow) (large arrows), besides some FB are Cav-3-positive but FAK-negative (small arrows) **(A–C)**. Some Cav-3-positive FB (red) are DDR-2-positive (green) and the two proteins are partially co-localized in FB tails (arrows) **(E–G)**. vWF-positive CEC (arrows) do not have Cav-3 **(I–K)**. ICLC are both Cav-3- (green) and c-Kit-positive (red) and the two proteins are partially co-localized (yellow) **(M–O)**. In Cav-$1^{-/-}$ mouse Cav-3 appeared at CM plasma membranes, **Z-lines** and FB (arrows), but FAK and c-Kit are completely absent **(D** and **P)**. DDR-2 and vWF shows at FB and CEC, respectively **(H** and **I)**. Scale bar is 10 μm for a–d and i–p, and 7 μm for e–g.

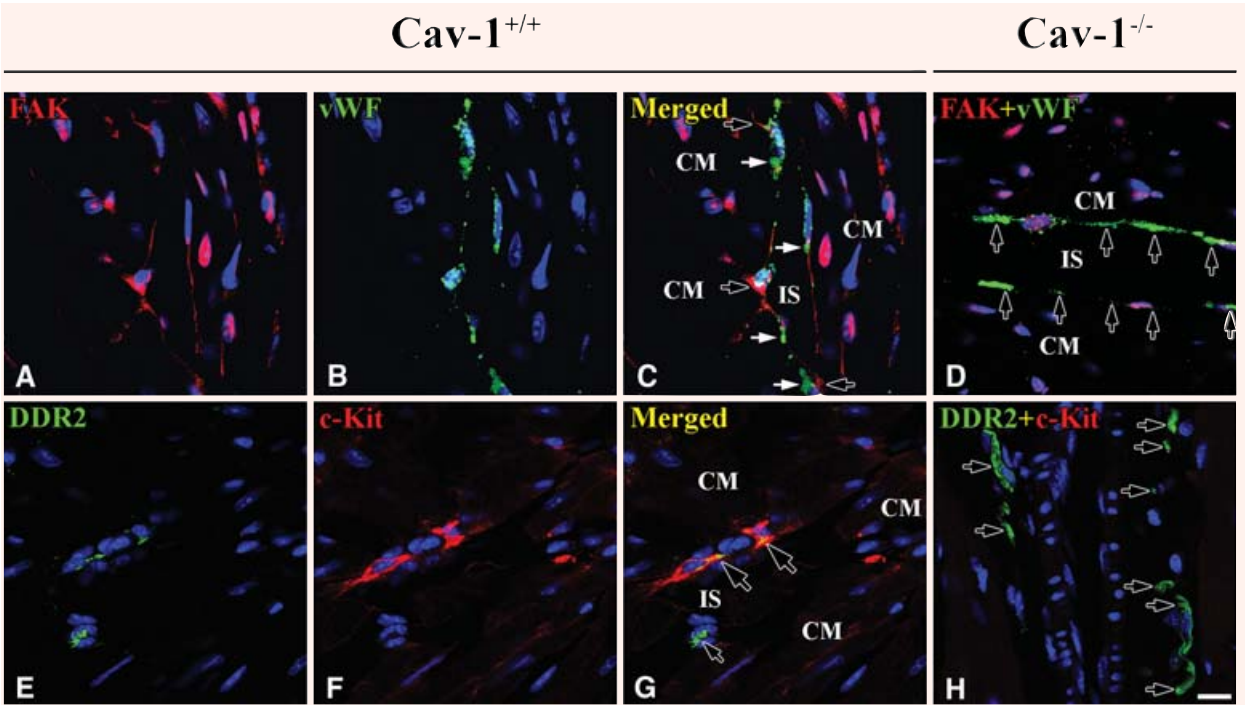

Fig. 7 Localization of FAK and vWF and co-localization of DDR-2 and c-Kit in Cav-1$^{+/+}$ and Cav-1$^{-/-}$ mouse LVM. In Cav-1$^{+/+}$ mouse FAK (red, open arrows) appears at FB and vWF (green, closed arrows) does at CEC, but these are not co-localized **(A–C)**. Interestingly some DDR-2-positive FB (green, small open arrow) are c-Kit-positive (red, small closed arrows) and these are partially co-localized (yellow, large open arrows) **(E–G)**. In Cav-1$^{-/-}$ mouse FAK is completely absent but vWF (green, arrows) appears at CEC **(D)**. c-Kit, also, is completely absent but DDR-2 (green, arrows) appears at FB **(H)**. CM is cardiomyocyte and IS is interstitial space. Scale bar is 10 μm for all images.

colemma and between masses of myofilaments. Spherical lipid droplets were often located between the ends of the mitochondria. Glycogen particles in the form of dense granules were crowded into the interstices among the mitochondria and near by Z-lines (Fig. 8A and B). In longitudinal sections of CM of Cav-1$^{-/-}$ mouse LVM CM revealed an abundance of large mitochondria and mass of myofilaments, as in control cells. However, a few opened Cav were present at the sarcolemma and some SR along sarcolemma was discontinuously located (Fig. 8D and E).

Capillary endothelial cell

Almost every CEC was located close to and between CMs. A number of opened and closed Cav were revealed at CEC membrane and cytoplasm, respectively, in Cav-1$^{+/+}$ mouse LVM (Fig. 8A and B). In Cav-1$^{-/-}$ mouse LVM location of CEC was similar to Cav-1$^{+/+}$ mouse LVM. Interestingly, some opened Cav appeared at CEC membrane and sometimes pericyte appeared near by CEC (Fig. 8D and E).

Fibroblasts

In general FB had two locations. One was between CM and CM or CM and CEC. The other was in the interstitial space and close to CM. FB revealed large nucleus in the centre of the cell and well-developed rough endoplasmic reticulum (rER) in the cytoplasm, but mitochondria was rare. We observed no open Cav, characteristically, in Cav-1$^{+/+}$ mouse LVM (Fig. 8B and C). In Cav-1$^{-/-}$ mouse LVM location of FB was similar to Cav-1$^{+/+}$ mouse LVM. FB revealed a similar distribution of micro-organelle to Cav-1$^{+/+}$ mouse LVM except, interestingly, a few open Cav appeared at FB membrane (Fig. 8E and F).

Discussion

Our major findings, summarized in Tables 3 and 4, in two-photon confocal microscopy were that: (1) MMP-2 expression depends upon Cav-1 expression in CM, FB

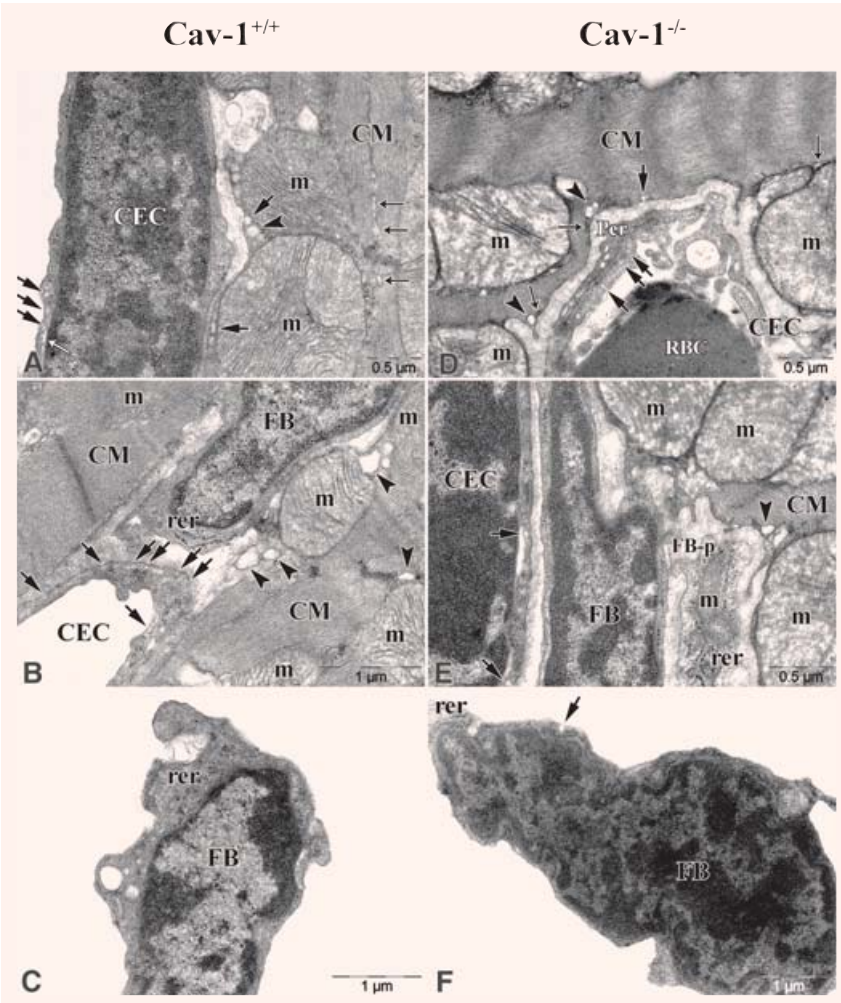

Fig. 8 Electron micrographs of CM, FB and CEC in Cav-$1^{+/+}$ and Cav-$1^{-/-}$ mouse LVM. In Cav-$1^{+/+}$ mouse **A–C** shows that CM, FB and CEC are closely located. Some caveolae (Cav, arrows) reveal at CM sarcolemma and a number of (Cav, arrows) reveal at CEC membrane. Well-developed sarcoplasmic reticulums (SR, closed thin arrows) are continuously arranged between myofilaments in CM and a few endoplasmic reticulums (ER, open thin arrows) reveal near by Cav at CEC membrane. Sacs of T-tubules (arrowheads) reveal adjacent to Cav and SR of CM and large mitochondria (m) locate adjacent to sarcolemma. FB does not have Cav but have well-developed rough ER. In Cav-$1^{-/-}$ mouse **D–F** shows that CM, FB and CEC are closely located as Cav-$1^{+/+}$ mouse. A few Cav (arrow) reveal at the sarcolemma and some flat-shaped SR (closed thin arrows) along the sarcolemma are discontinuously located in CM. Sacs of T-tubules (arrowheads) reveal adjacent to SR. CEC have a few Cav. FB does not have Cav, but a few have it. FB-p, process of fibroblast.

and CEC; (2) Cav-2 expression does not depend upon Cav-1 expression in CEC; (3) Cav-3 expression does not depend upon Cav-1 expression in CM and FB; (4) FAK expression depends upon Cav-1 expression in FB and (5) c-Kit expression depends upon Cav-1 expression in ICLC.

Co-expression of MMP-2 and Cav-1 at CM membrane and Z-lines supports our recent report [16] and confirms previous reports of sarcomeric association in the heart [15]. Clearly also MMP-2 expression depends upon Cav-1 expression based on diminished MMP-2 expression in Cav-$1^{-/-}$ LVM. In CM, Cav-1 expression was continuous and not punctate at and along CM membrane. This pattern of Cav-1 expression is different from Cav-1 expression at the membrane of intestinal SMC membranes and ICC where it was punctate in the PM [19, 24]. Cav formation in smooth muscle depends on expression of Cav-1 and Cav are usually arranged in rows aligned with the long axes of cells. Therefore when these cells are cut in cross sections, immunoreactivity associated with Cav occurs in punctate fashion. In contrast, Cav-1 is not present in all Cav at CM membrane and Cav were not present in a regular pattern. Also, molecules of Cav-1 at CM membrane may exist in non-caveolar lipid raft; *i.e.* individual Cav-1 molecules may exist at CM membranes not associated with Cav.

Cav-2 expression occurred only at CEC and regardless of Cav-1 expression in mouse LVM. This finding differs from our previous report that Cav-2

Table 3 Co-localization between proteins in Cav-1$^{+/+}$ mouse left ventricular myocardium

Proteins	CM			CEC	FB	ICLC
	PM	z-line	MF			
MMP-2 + Cav-1	+++	+	+	+++	+++	n/a
MMP-2 + Cav-2	-	-	-	+++	-	n/a
MMP-2 + Cav-3	+++	+++	+++	++	+	n/a
MMP-2 + FAK	-	-	-	-	+++	n/a
MMP-2 + DDR2	-	-	-	-	+++	-
MMP-2 + vWF	-	-	-	+++	-	-
MMP-2 + c-Kit	-	-	-	-	+/-	+++
Cav-1 + Cav-2	-	-	-	+	-	n/a
Cav-1 + Cav-3	++	+	+	++	+	n/a
Cav-2 + Cav-3	-	-	-	++	-	n/a
Cav-1 + FAK	-	-	-	-	+++	n/a
Cav-1 + vWF	-	-	-	+++	-	-
Cav-1 + DDR2	-	-	-	-	+++	-
Cav-1 + c-Kit	-	-	-	-	+/-	+++
Cav-2 + FAK	-	-	-	-	-	n/a
Cav-2 + c-Kit	-	-	-	-	-	-
Cav-3 + FAK	-	-	-	-	++	n/a
Cav-3 + DDR2	-	-	-	-	+	-
Cav-3 + vWF	-	-	-	-	-	-
Cav-3 + c-Kit	-	-	-	-	+/-	++
FAK + vWF	-	-	-	-	-	-
DDR2 + c-Kit	-	-	-	-	+/-	+/-

CM, cardiomyocytes; FB, fibroblasts; CEC, capillary endothelial cells; ICLC, interstitial Cajal-like cells; PM, plasma membranes; MF, myofilaments; MMP-2, matrix metalloprotenase-2; Cav-1, caveolin-1; Cav-2, caveolin-2; Cav-3, caveolin-3; FAK, focal adhesion kinase; DDR2, discoidin domain receptor-2; vWF, von Willebrand factor; c-Kit, receptor tyrosine kinase; +, ++ and +++ indicate immunoreactive intensity; - means absent or inconspicuous; +/- means present occasionally.

expression depended completely upon Cav-1 expression in intestinal SMC and ICC [24]. These findings suggest that Cav-2 expression may be differently controlled, possibly aided by the presence of Cav-3, depending on tissue specificity.

According to our previous report, Cav-3 expression appeared diminished in outer circular muscle when Cav-1 was missing in intestinal SMC and ICC [24]. In the heart, however, Cav-3 expression was not dependent upon Cav-1 and occurred essentially unchanged in Cav-1$^{-/-}$ mouse LVM. Thus, Cav-3 expression is not dependent on Cav-1 expression in CM, Z-lines and FB. The pattern of Cav-3 expression was punctate at CM membrane at Z-lines and diffuse over FB.

In ultrastructural observation Cav were present at CM membrane in Cav-1$^{-/-}$ mouse LVM. This finding supports previous reports that Cav-3, by itself, has the capability to form Cav [25].

Table 4 Co-localization between proteins in Cav-1$^{-/-}$ mouse left ventricular myocardium

Proteins	CM			CEC	FB	ICLC
	PM	z-line	MF			
MMP-2 + Cav-1	-	-	-	-	-	n/a
MMP-2 + Cav-2	-	-	-	-	-	n/a
MMP-2 + Cav-3	-	+/-	+/-	+/-	-	n/a
MMP-2 + FAK	-	-	-	-	-	n/a
MMP-2 + DDR2	-	-	-	-	-	-
MMP-2 + vWF	-	-	-	-	-	-
MMP-2 + c-Kit	-	-	-	-	-	-
Cav-1 + Cav-2	-	-	-	-	-	n/a
Cav-1 + Cav-3	-	-	-	-	-	n/a
Cav-2 + Cav-3	-	-	-	+	+	n/a
Cav-1 + FAK	-	-	-	-	-	n/a
Cav-1 + vWF	-	-	-	-	-	-
Cav-1 + DDR2	-	-	-	-	-	-
Cav-1 + c-Kit	-	-	-	-	-	-
Cav-2 + FAK	-	-	-	-	-	n/a
Cav-2 + c-Kit	-	-	-	-	-	-
Cav-3 + FAK	-	-	-	-	-	n/a
Cav-3 + DDR2	-	-	-	-	+	-
Cav-3 + vWF	-	-	-	-	-	-
Cav-3 + c-Kit	-	-	-	-	-	-
FAK + vWF	-	-	-	-	-	-
DDR2 + c-Kit	-	-	-	-	-	-

CM, cardiomyocytes; FB, fibroblasts; CEC, capillary endothelial cells; ICLC, interstitial Cajal-like cells; PM, plasma membranes; MF, myofilaments; MMP-2, matrix metalloprotenase-2; Cav-1, caveolin-1; Cav-2, caveolin-2; Cav-3, caveolin-3; FAK, focal adhesion kinase; DDR2, discoidin domain receptor-2; vWF, von Willebrand factor; c-Kit, receptor tyrosine kinase; +, ++ and +++ indicate immunoreactive intensity; - means absent or inconspicuous; +/- means present occasionally.

FB is involved in wound healing after myocardial infarction leading to heart failure [26, 27] and the FAK is known as a factor which regulates cell adhesion and migration [28]. Our study showed that FAK is associated with MMP-2 as well as Cav-1 based on co-expression in FB of Cav-1$^{+/+}$ LVM and on the loss of both in Cav-1$^{-/-}$ FB. FAK expression, therefore, apparently depends upon Cav-1 expression in FB; moreover MMP-2 could become active in wound healing and Cav-1 could provide an anchoring site for the actin cytoskeleton that control FB morphology [29].

Popescu and co-workers reported the presence of ICLC in the rat LVM, based on their ultrastructure. They had some Cav, poorly-developed rER and veil-like long processes, and were distinguished from FB through ultrastructurally comparisons [5]. We wondered of these ICLC were labelled with c-Kit. c-Kit, tyrosine receptor kinase, is necessary for the development of haematopoietic progenitor and mast cells,

and also FB and ICC originating from mesenchymal cells [27]. In our finding, c-Kit was co-expressed with MMP-2, Cav-1 and Cav-3 in ICLC of Cav-$1^{+/+}$ LVM, but surprisingly not in Cav-$1^{-/-}$ LVM. c-Kit expression depends upon Cav-1 expression in ICLC and it could be regulated with Cav-1 during development of the heart. This was not the case in Cav-$1^{-/-}$ mouse intestine, which expressed c-Kit in ICC despite the absence of Cav-1 [24].

In conclusion expression / co-expression of MMP-2, Cav-1, FAK and c-Kit is crucially associated with one another in CM, FB and CEC of the myocardium. These further immunohistochemical and electron microscopic findings suggest that the roles of Cav-1 and MMP2 extend beyond the CM and that endothelial and FB like cells may also play a role in the responses to myocardial infarction and ischaemia.

Acknowledgements

This work was supported by a grant from the Heart and Stroke Foundation of Canada and a Pharmacology Research Grant.

References

1. **Camelliti P, McCulloch AD, Kohl P.** Microstructured cocultures of cardiac myocytes and fibroblasts: a two-dimensional *in vitro* model of cardiac tissue. *Microsc Microanal.* 2005; 11: 249–59.
2. **Camelliti P, Borg TK, Kohl P.** Structural and functional characterisation of cardiac fibroblasts. *Cardiovascular Res.* 2005; 65: 40–51.
3. **Voldstedlund M, Vinten J, Tranum-Jensen J.** cav-p60 expression in rat muscle tissues distribution of caveolar proreins. *Cell Tissue Res.* 2001; 306: 265–76.
4. **Hinescu ME, Gherghiceanu M, Mandache E, Ciontea SM, Popescu LM.** Interstitial Cajal-like cells (ICLC) in atrial myocardium: ultrastructural and immunohistochemical characterization. *J Cell Mol Med.* 2006; 10: 243–57.
5. **Popescu LM, Gherghiceanu M, Hinescu ME, Cretoiu D, Ceafalan L, Regalia T, Porescu AC, Ardeleanu C, Mandache E.** Insights into the interstitium of ventricular myocaedium: interstitial Cajal-like cells (ICLC). *J Cell Mol Med.* 2006; 10: 429–58.
6. **Chen YJ, Li Y, Zhang P, Traverse JH, Hou M, Xu X, Kimoto M, Bache RJ.** Dimethylarginine dimethylaminohydrolase and endothelial dysfunction in failing hearts. *Am J Physiol Heart Circ Physiol.* 2005; 289: H2212–9.
7. **Feron O, Belhassen L, Kobzik L, Smith TW, Kelly RA, Michel T.** Endothelial nitric oxide synthase targeting to caveolae. *J Biol Chem.* 1996; 271: 22810–4.
8. **Goldsmith EC, Hoffman A, Morales MO, Potts JD, Price RL, McFadden A, Rice M, Borg TK.** Organization of fibroblasts in the heart. *Dev Dyn.* 2004; 230: 787–94.
9. **Laframboise WA, Scalise D, Stoodley P, Graner SR, Guthrie RD, Magovern JA, Becich MJ.** Cardiac fibroblasts influence cardiomyocyte phenotype *in vitro*. *Am J Physiol Cell Physiol.* 2007; 292: C1799–808.
10. **Swaney JS, Patel HH, Yokoyama U, Head BP, Roth DM, Insel PA.** Focal adhesions in (myo) fibroblasts scaffold adenylyl cyclase with phosphorylated caveolin. *J Biol Chem.* 2006; 281: 17173–9.
11. **Preissner KT, Pötzsch B.** Vessel wall-dependent metabolic pathways of the adhesive proteins, von-Willebrand-factor and vitronectin. *Histol Histopathol.* 1995; 10: 239–51.
12. **Makkar RR, Price MJ, Lill M, Frantzen M, Takizawa K, Kleisli T, Zheng J, Kar S, McClelan R, Miyamota T, Bick-Forrester J, Fishbein MC, Shah PK, Forrester JS, Sharifi B, Chen PS, Qayyum M.** Intramyocardial injection of allogenic bone marrow-derived mesenchymal stem cells without immunosuppression preserves cardiac function in a porcine model of myocardial infarction. *J Cardiovasc Pharmacol Therapeut.* 2005; 10: 225–33.
13. **Lalu MM, Wang W, Schulz R.** Peroxynitrite in Myocardial ischemia-reperfusion injury. In: Jugdutt BI. editor. Role of Nitric Oxide in Heart Failure. Hingham, MA, USA: Kluwer Academic Publishers; 2004. pp. 201–11.
14. **Wang W, Schulze CJ, Suarez-Pinzon WL, Dyck JR, Sawicki G, Schulz R.** Intracellular action of matrix metalloproteinase-2 accounts for acute myocardial ischemia and reperfusion injury. *Circulation.* 2002; 106: 1543–9.
15. **Sawicki G, Leon H, Sawicka J, Sariahmetoglu M, Schulze CJ, Scott PG, Szczesna-Cordary D, Schulz R.** Degradation of myosin light chain in isolated rat hearts subjected to ischemia-reperfusion injury: a new intracellular target for matrix metalloproteinase-2. *Circulation.* 2005; 112: 544–52.
16. **Chow AK, Cena J, El-Yazbi AF, Crawford BD, Holt A, Cho WJ, Daniel EE, Schulz R.** Caveolin-1 inhibits matrix metalloproteinase-2 activity in the heart. *J Mol Cell Cardiol.* 2007; 42: 896–901.
17. **Puyraimond A, Fridman R, Lemesle M, Arbeille B, Menashi1 S.** MMP-2 colocalizes with caveolae on

the surface of endothelial cells. *Exp Cell Res.* 2001; 262: 28–36.
18. **Head BP, Insel PA.** Do caveolins regulate cells by actions outside of caveolae? *Trends in Cell Biol.* 2007; 17: 51–7.
19. **Daniel EE, Bodie G, Mannario M, Boddy G, Cho WJ.** Changes in membrane cholesterol affect caveolin-1 localization and ICC-pacing in mouse jejunum. *Am J Physiol Gastrointest Liver Physiol.* 2004; 287: G202–10.
20. **El-Yazbi AF, Cho WJ, Boddy G, Daniel EE.** Caveolin-1 gene knockout impairs nitrergic function in mouse small intestine. *Br J Pharmacol.* 2005; 145: 1017–26.
21. **El-Yazbi AF, Cho WJ, Boddy G, Shultz R, Daniel EE.** The impact of caveolin-1 knockout on NANC relaxation in circular muscles of mouse small intestine compared to longitudinal muscles. *Am J Physiol Gastrointest Liver Physiol.* 2006; 290: G394–403.
22. **Darby PJ, Daniel EE.** Caveolae from canine airway smooth muscle contain the necessary components for a role in Ca^{2+}-handling. *Am J Physiol Lung Cell Mol Physiol.* 2000; 279: L1226–35.
23. **Daniel EE, Jury J, Wang YF.** nNOS canine lower esophageal sphincter: colocalized with Cav1 and Ca^{2+}-handling proteins? *Am J Physiol Gastrointest Liver Physiol.* 2001; 281: G1101–14.
24. **Cho WJ, Daniel EE.** Colocalization between caveolin isoforms in the intestinal smooth muscle and interstitial cells of Cajal of the $Cav1^{+/+}$ and $Cav1^{-/-}$ mouse. *Histochem Cell Biol.* 2006; 126: 9–16.
25. **Park DS, Woodman SE, Schubert W, Cohen AW, Frank PG, Chandra M, Shirani J, Razani B, Tang B, Jelicks LA, Factor SM, Weiss LM, Tanowitz HB, Lisanti MP.** Caveolin-1/3 double-knockout mice are viable, but lack both muscle and non-muscle caveolae, and develop a severe cardiomyopathic phenotype. *Am J Pathol.* 2002; 160: 2207–17.
26. **Squires CE, Escobar GP, Payne JF, Leonardi RA, Goshorn DK, Sheats NJ, Mains IM, Mingoia JT, Flack EC, Lindsey ML.** Altered fibroblast function following myocardial infarction. *J Mol Cell Cardiol.* 2005; 39: 699–707.
27. **Möllmann H, Nef HM, Kostin S, von Kalle C, Pilz I, Weber M, Schaper J, Hamm CW, Elsässer A.** Bone marrow-derived cells contribute to infarct remodelling. *Cardiovasc Res.* 2006; 71: 661–71.
28. **Hakuno D, Takahashi T, Lammerding J, Lee RT.** Focal adhesion kinase signaling regulates cardiogenesis of embryonic stem cells. *J Biol Chem.* 2005; 280: 39534–44.
29. **Swaney JS, Patel HH, Yokoyama U, Head BP, Roth DM, Insel PA.** Focal adhesions in (myo) fibroblasts scaffold adenylyl cyclase with phosphorylated caveolin. *J Biol Chem.* 2006; 281: 17173–9.